Available online at www.sciencedirect.com
ScienceDirect
Tetrahedron: *Asymmetry* 19 (2008) 1084–1093
Tetrahedron: *Asymmetry*

# Chiral discrimination processes by C9 carbamate derivatives of dihydroquinine: interaction mechanisms of diastereoisomeric 9-*O*-[(*S*)- or (*R*)-1-(1-naphthyl)ethylcarbamate]dihydroquinine and the two enantiomers of *N*-(3,5-dinitrobenzoyl)alanine methyl ester

Gloria Uccello-Barretta,[a,*] Federica Balzano,[a] Silvia Bardoni,[a] Letizia Vanni,[a] Laura Giurato[b] and Salvatore Guccione[b,*]

[a] *Università degli Studi di Pisa, Dipartimento di Chimica e Chimica Industriale, Via Risorgimento 35, I-56126 Pisa, Italy*
[b] *Università degli Studi di Catania, Dipartimento di Scienze Farmaceutiche, Città Universitaria Ed. 2, Viale A. Doria 6, I-95125 Catania, Italy*

Received 11 March 2008; accepted 8 April 2008
Available online 13 May 2008

**Abstract**—Computational and NMR investigations of diastereoisomeric aggregates arising from the interaction of 9-*O*-[(*S*)- or (*R*)-1-(1-naphthyl)ethylcarbamate]dihydroquinine and the two enantiomers of *N*-(3,5-dinitrobenzoyl)alanine methyl ester pointed out the origin of chiral discrimination phenomena occurring in $CDCl_3$ solutions.


## 1. Introduction

C9 carbamoyl derivatives of quinine have gained popularity as chiral selectors for chromatography[1] and as chiral solvating agents (CSAs) for NMR spectroscopy.[2] In attempting to improve the applications in this latter field, we pointed out their efficiency and widespread applicability to the NMR enantiodiscrimination of π-acidic derivatives of chiral substrates and recognized some of their structural requirements for enantiodiscrimination to occur: the presence of an aromatic moiety on the carbamate function, which is able to produce enhanced NMR anisochrony when separated from the NH by a carbon atom and, importantly, the role of the presence of an additional stereogenic centre introduced together with the carbamoyl group.[2a–c] In particular, 9-*O*-[(*S*)-1-(1-naphthyl)ethylcarbamate]dihydroquinine **1** (Scheme 1) showed a high efficiency in the NMR enantiodiscrimination of several kinds of chiral substrates, markedly superior to that of its diastereoisomer **2** having an opposite absolute configuration at the carbamoyl function.[2b]

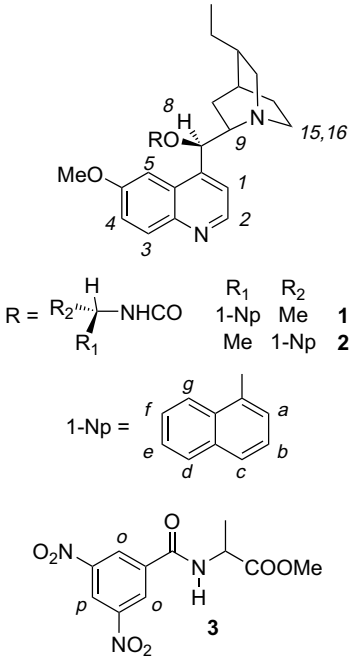


**Scheme 1.** CSAs **1** and **2** and α-amino acid derivative **3**.

* Corresponding authors. Fax: +39 0502219260 (G.U.-B); Fax: +39 095443604 (S.G); e-mail addresses: gub@dcci.unipi.it; guccione@unict.it

0957-4166/$ - see front matter © 2008 Elsevier Ltd. All rights reserved.
doi:10.1016/j.tetasy.2008.04.009

In order to rationalize the above differences between **1** and **2**, we carried out a combined and accurate NMR-molecular modelling investigation of the molecular basis of chiral discrimination by the diastereoisomeric C9 carbamates **1** and **2** on considering as a probe chiral substrate (*R*)- or (*S*)-*N*-(3,5-dinitrobenzoyl)alanine methyl ester **3** (Scheme 1). This last chiral substrate, endowed with a π-acidic aromatic ring and only one potential hydrogen bond donor group, concomitantly gave us the opportunity of complementing our previous investigations[2a,d] involving enantiomeric substrates having two different types of hydrogen bond donor groups, in order to complete the picture of chiral recognition processes by C9 carbamates of dihydroquinine. Computational studies were undertaken in order to shed further light on the stereodiscrimination mechanisms, the conformational preferences and the origin of the binding selectivities experimentally determined by NMR.

## 2. Results and discussion

Between 2 and 500 mM concentrations, NMR parameters of the diastereoisomeric chiral selectors **1** and **2** did not show significant variations and, hence, we could neglect self-association phenomena, which, on the contrary, were detected in underivatized quinine[3] or in a lower extent for its carbamoyl derivatives with the aromatic moiety directly bound to the NH.[2a] In $CDCl_3$, spectra of **1** and **2** revealed the presence of two species in 90 to 10 ratio (Figure S1, Supporting Information), due to the *anti* and *syn* stereoisomers, respectively. As already reported for carbamates,[4] their mutual slow interconversion involves the rotation about the NH–CO bond, which was clearly demonstrated here by the presence of exchange peaks between the corresponding signals of the two species in the NOESY maps.

The $^1$H NMR signals of the major *anti*-stereoisomers of **1** and **2** were completely assigned (see Section 4), whereas only some resonances of the minor ones were attributed by exchange peaks produced in the 2D NOESY maps with these known signals of *anti*-stereoisomers.

As already observed for the carbamoyl or estereal derivatives of quinines,[2a] compounds **1** and **2** were present in solution as strongly prevailing *closed* conformers with the quinuclidine nitrogen pointing at the quinoline ring and $H_8$ proton pointing at $H_5$ quinoline proton (Fig. 1). As a matter of fact interNOE $H_9$–$H_5$ was less intense than $H_9$–$H_1$ one was (Fig. 2a and b), and interNOE $H_8$–$H_9$ was less intense than interNOE $H_8$–$H_{15}$ (Fig. 2c and d). Prevailing orientation of the $H_8$ proton is demonstrated on the basis of comparison of interNOEs $H_8$–$H_5$ and $H_8$–$H_1$ (Fig. 2c and d).

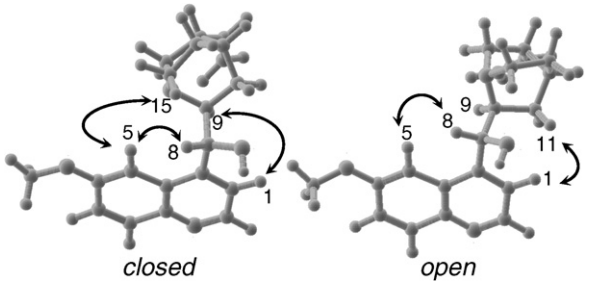


**Figure 1.** Graphical representation of the *open* and the *closed* conformers of quinine.

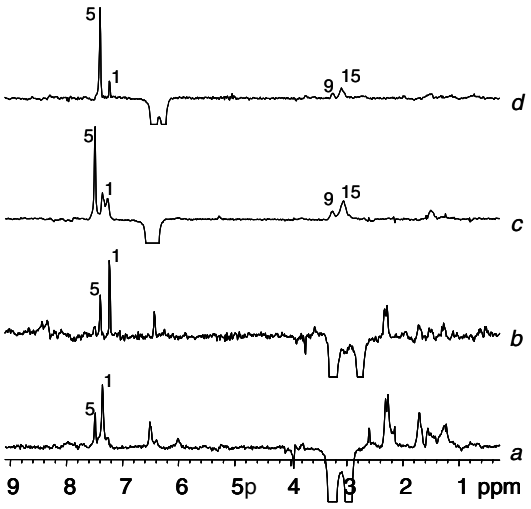


**Figure 2.** 2D NOESY (300 MHz, $CDCl_3$, 120 mM, 25 °C, mix = 0.6 s) traces corresponding to $H_9$ protons of **1** (a) and **2** (b) and traces corresponding to $H_8$ protons of **1** (c) and **2** (d).

Inside the carbamoyl function, the 1-(1-naphthyl)ethyl portion has the same conformation in **1** and **2**, in fact its methine proton (Fig. 3a) originated from strongly prevalent dipolar interactions with the adjacent peri proton $H_g$, whereas both the NH (Fig. 3b) and methyl groups (Fig. 3c) gave intense NOEs at the frequency of the naphthyl β-proton named $H_a$. Furthermore, no significant NH–CH dipolar interaction was detected (Fig. 3a and b), therefore, the NH and CH bonds were *transoid*. This is also in keeping with the value of 145° calculated for the dihedral angle H–N–C–H from the vicinal coupling constant $^3J_{NH-CH}$ of 7.7 Hz on the basis of Karplus relationship.[5] Thus, we conclude that the CH bond is coplanar to the naphthyl moiety and points at the

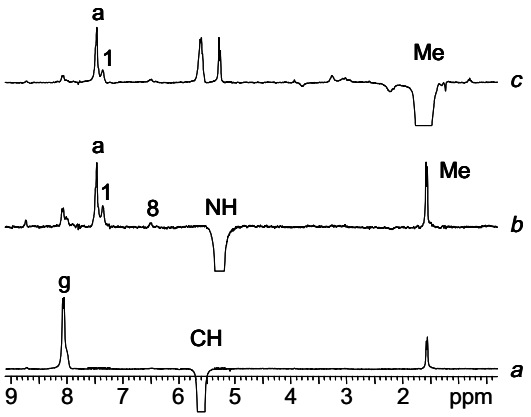


**Figure 3.** $^1$H{$^1$H}-NOE difference spectra (300 MHz, $CDCl_3$, 25 °C) of **1** (120 mM) corresponding to the saturation of CH (a), NH (b) and Me (c) protons.

peri proton $H_g$, whereas the NH and methyl groups lie on the opposite sides of the naphthalene ring, nearer to the proton $H_a$ than they are to the $H_g$ one (Fig. 4). In this way, the NH bond is *cisoid* to the methyl group and, thus the corresponding intense dipolar interaction in its NOE spectrum is detected (Fig. 3b).

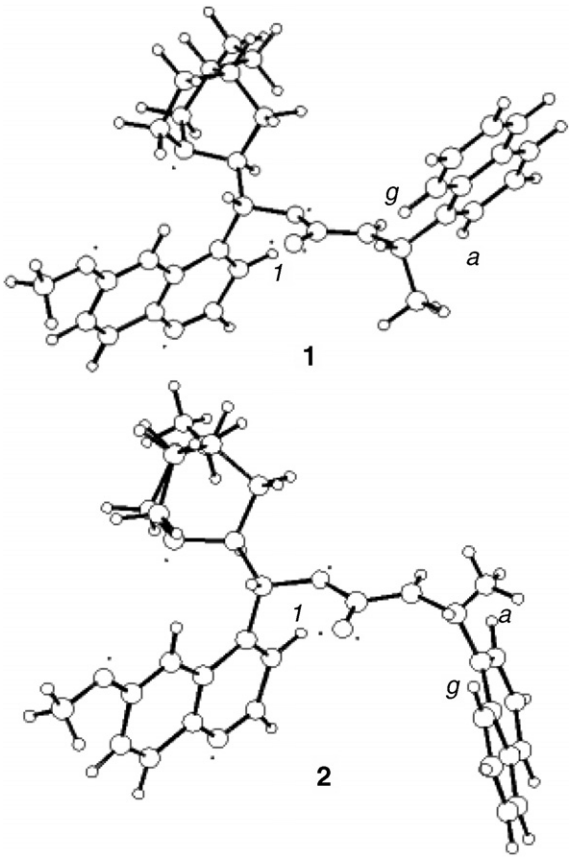


**Figure 4.** Graphical representation of the *anti*-conformers of **1** and **2**.

Finally, the relative position of the carbamoyl function and quinine moiety must be defined: NOEs caused by perturbing at the NH frequencies of **1** and **2** were diagnostic to this respect. In fact, interNOE NH–$H_1$ was greater than NH–$H_8$ interNOE (Fig. 3b), therefore the NH bond of the carbamate function must be *transoid* to the $H_8$ proton, pointing at the quinoline proton $H_1$ (Fig. 4). In this way, the stereochemistry of **1** or **2** was completely defined on the basis of the knowledge of the prefixed absolute configuration of the new stereogenic center. In fact, in **1**, in which its absolute configuration is (*S*), the naphthyl ring must be *transoid* to the quinoline ring and, hence, *syn* with respect to the quinuclidine moiety while its methyl group must be on the same side of the quinoline moiety (Fig. 4). However, both the methyl group and naphthalene ring are far away from dihydroquinine structure as no NOEs with the quinoline or quinuclidine portion were detected.

In diastereosiomer **2**, in which the (*R*)-1-(1-naphthyl)ethyl moiety was present, the naphthyl and quinoline plane are *syn* and the methyl group *anti* with respect to it and, hence, faced to the quinuclidine ring (Fig. 4). The interchange of methyl and naphthyl groups in **1** and **2** is well reflected in some differences found in their chemical shifts: $H_1$ and $H_2$ protons of the quinoline ring of **2** and the $H_g$ and $H_a$ protons of its naphthalene ring are significantly low-frequency shifted with respect to **1** (Table 1), as expected on the basis of the reciprocal anisotropic effects of *syn* quinoline and naphthalene rings of **2**.

**Table 1.** Chemical shift data (300 MHz, $CDCl_3$, 25 °C, $\delta$ in ppm referenced to TMS as external standard) of some protons of *anti* conformers of **1** and **2** (120 mM)

| | **1** | **2** |
|---|---|---|
| $H_1$ | 7.35 | 7.24 |
| $H_2$ | 8.72 | 8.63 |
| $H_a$ | 7.47 | 7.37 |
| $H_g$ | 8.08 | 7.81 |
| Me | 1.57 | 1.64 |

The average conformation of **3** (Fig. 5) was defined on the basis of the value of 143° for the dihedral angle H–C–N–H calculated from the vicinal coupling constant $^3J_{NH-CH}$ of 7.2 Hz. This is according to the *transoid* NH–CH arrangement with the ester function bent at the NH bond (Fig. 5) as determined by the absence of NH–CH NOE and the detection of dipolar interaction between the ester group and the NH proton.

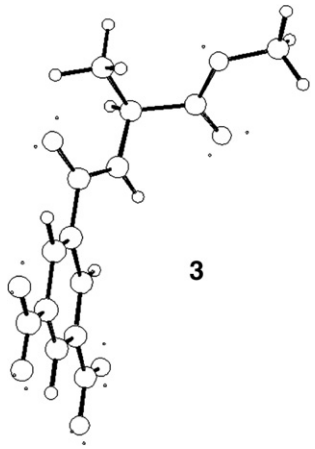


**Figure 5.** Graphical representation of (*S*)-**3**.

As already discussed,[2b] the carbamate dihydroquinine **1** enantiodiscriminated the amino acid derivative **3** with very high efficiency ($\Delta\delta = 86.0$ Hz for the methyl signal), whereas the nonequivalences measured in the presence of its diastereoisomer **2** were significantly lower ($\Delta\delta = 5.6$ Hz for the methyl signal). Therefore, we proceeded to analyse the equimolar mixtures formed by **1** or **2** and the two enantiomers of **3**, starting from the determination of their complexation parameters. The complexation stoichiometries were always 1 to 1 as found by using the continuous variation Job method,[6] which involved the analysis of mixtures with constant total concentration, but different molar fractions of the two components.

Among the different methods reported for the determination of the association constants of 1 to 1 complexes,[7] a

useful alternative to the Benesi–Hildebrand derived method involves the determination of the chemical shifts of progressively diluted (240–2 mM) equimolar chiral auxiliary/substrate solutions and the non-linear fitting of equation (see Section 4), which describes the dependence of the chemical shifts on the concentration. The above method could be employed in virtue of the fact that self-aggregation processes are unimportant for **1** and **2**. In this way, for the two diastereoisomeric complexes **1**/(*S*)-**3** and **1**/(*R*)-**3** we found the values of $12.3 \pm 1.6\ M^{-1}$ and $5.9 \pm 0.4\ M^{-1}$, respectively, whereas no significative difference of the association constants of the two diastereoisomers **2**/(*S*)-**3** and **2**/(*R*)-**3** was found ($K = 5.2 \pm 0.4\ M^{-1}$ for **2**/(*S*)-**3** and $K = 6.7 \pm 0.6\ M^{-1}$ for **2**/(*R*)-**3**).

The determination of the relative stereochemistry of each enantiomer of **3** and the two diastereoisomeric carbamates **1** and **2**, as obtained by detecting the intermolecular NOEs in their mixtures, gave full account of these data. The following NOEs were detected in the equimolar mixture **1**/(*S*)-**3,** at a very high total concentration (240 mM) (in order to have a relevant percentage of the two components in the bound state): (a) dipolar interaction between the naphthalene peri protons $H_c$ and $H_d$ of **1** and both aromatic protons $H_p$ and $H_o$ of the 3,5-dinitrophenyl ring of **3** (Fig. 6a), with the effect detected on the para proton more intense with respect to that one produced on the $H_o$ nuclei; (b) the partially superimposed NH and CH protons of the 1-(1-naphthyl)ethyl group originated dipolar interactions with the two above protons, $H_o$ and $H_p$, but, in this case, the more intense effect was detected at the *ortho*-protons of the π-acidic moiety (Fig. 6b); (c) furthermore, the perturbation of dihydroquinine proton $H_8$ was able to affect the intensity of the ortho and NH protons of **3** (Fig. 6c); (d) methine proton of **3** bound to the chiral carbon atom produced only the expected intramolecular NOEs, whereas any intermolecular effect was not detected (Fig. 6d). By contrast its methyl protons gave an intense NOE at the frequency of the quinoline proton $H_3$ and a minor effect at the frequency of $H_2$ (Fig. 6e). The above data allowed us to define very precisely the relative orientations of **1** and (*S*)-**3** in the complex. In fact the 3,5-dinitrophenyl ring of (*S*)-**3** is included in the pocket determined by the quinuclidine and naphthyl moieties of the carbamate function of **1**: its para proton is in the direction of the peri protons $H_c$ and $H_d$ and its ortho protons are directed towards quinine $H_8$ proton. The same proton $H_8$ is also found in the spatial proximity of the NH group of **3**. The methine proton of (*S*)-**3** is external to the molecular adduct, whereas its methyl group points towards the $H_3$ quinoline proton as in Figure 7.

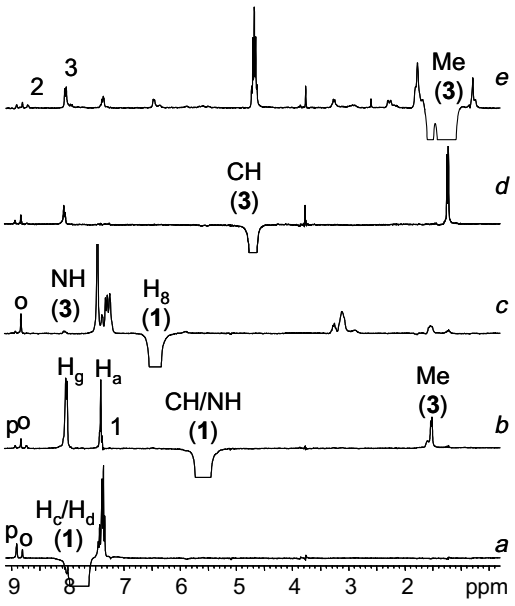


**Figure 6.** $^1H\{^1H\}$-NOE difference spectra (300 MHz, $CDCl_3$, 25 °C) of equimolar mixture (*S*)-**3**/**1** (120 mM) corresponding to the saturation of $H_c$ and $H_d$ (a), NH + CH (b) and $H_8$ (c) protons of **1** and of CH (d) and Me (e) protons of (*S*)-**3**.

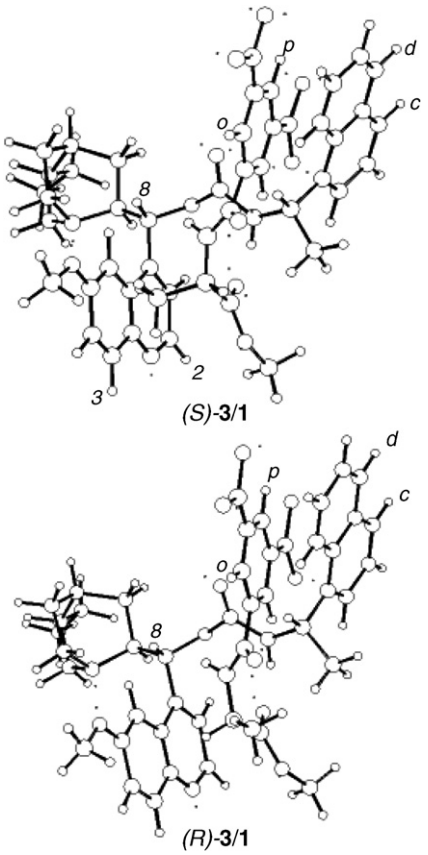


**Figure 7.** Graphical representation of the diastereoisomeric complexes (*S*)-**3**/**1** and (*R*)-**3**/**1**.

Therefore, the **1**/(*S*)-**3** adduct is stabilized by two simultaneous cooperating attractive interactions: the π–π interaction between the π-acidic ring of (*S*)-**3** and the naphthalene of the carbamate function and hydrogen bond interaction between the NH proton of (*S*)-**3** and the oxygen or carbonyl function of the carbamate.

The positions of the groups bound to the stereogenic center of (*S*)-**3** relative to **1**, which are unexpected at a first glance, can be well rationalized by considering that this arrangement allows a further attractive interaction between the

ester carbonyl of (*S*)-**3** and the carbamate NH proton and simultaneously allows methyl groups of (*S*)-**3** and 1-(1-naphthyl)ethyl moiety of **1** to be *transoid* each other.

NOE measurements carried out in mixtures **1**/(*R*)-**3** gave analogous results: the saturation of the naphthalene peri protons $H_c$ and $H_d$ of **1** originated comparable NOEs at the frequencies both of the $H_o$ and $H_p$ 3,5-dinitrophenyl protons of (*R*)-**3**, whereas the NH and CH protons of the carbamate function of **1** originated dipolar interactions with the $H_o$ protons of (*R*)-**3**, which was more intense relative to the same effect detected on $H_p$. Furthermore, the NH proton of the amino acid derivative originated dipolar interaction with the carbamate NH and CH protons and the dihydroquinine $H_8$ proton. Therefore, the orientation of (*R*)-**3** relatively to **1** is the same found for the (*S*)-enantiomer, that is, the 3,5-dinitrophenyl moiety is located in the spatial region included between the quinuclidine and the naphthalene rings faced to the latter one with its NH proton pointing at the NH and CH and $H_8$ protons of the chiral auxiliary. In this case any relevant dipolar interaction was detected between the methyl group of (*R*)-**3** and the protons of the chiral auxiliary: on the hypothesis that the methyl ester group is once again bent at the carbamate NH, we should have an interchange of the methyl and methine positions with respect to the previous case, therefore the methyl group of (*R*)-**3** is, in this case, *cisoid* to the methyl group of the carbamate function (Fig. 7).

Comparison of the complexation shift of **3** in the two complexes **1**/(*S*)-**3** and **1**/(*R*)-**3** (Table 2) strongly supports the above conclusions, in fact the NH proton of **3** undergoes a relevant high-frequencies shift ($\Delta\delta_S = 227.4$ Hz, $\Delta\delta_R = 198.7$ Hz), which is due to the hydrogen bond interaction with the carbamate carbonyl or oxygen. Due to the fact that the two protons are in the same stereochemical arrangement in both complexes, as revealed by NOEs, their NH chemical shift differentiation can be reliably attributed to the different stabilities of the two diastereoisomeric complexes.

**Table 2.** Complexation shifts ($\Delta\delta$[a], Hz, 300 MHz, $CDCl_3$, 25 °C) of **3** in the equimolar mixtures (120 mM) **1**/(*S*)-**3**, **1**/(*R*)-**3** and **2**/(*S*)-**3**, **2**/(*R*)-**3**

| | **1**/(*S*)-**3** | **1**/(*R*)-**3** | **2**/(*S*)-**3** | **2**/(*R*)-**3** |
|---|---|---|---|---|
| NH | 227.4 | 198.7 | 181.2 | 173.8 |
| $CH_3$ | −97.1 | −21.0 | −18.7 | −11.4 |

[a] $\Delta\delta = \delta_{mix} - \delta_{free}$; $\delta_{mix}$ = observed chemical shift measured in the mixture, $\delta_{free}$ = chemical shift of the pure compound.

No significant conformational change of **3** is observed as a consequence of the complexation.

Finally, the methyl group of (*S*)-**3** undergoes a low-frequency shift of about 100 Hz in the presence of **1** (Table 2), which can be attributed to the anisotropy of the quinoline ring towards which it is oriented.

In the complex **1**/(*R*)-**3** the same group undergoes a remarkably lower shielding (about 21 Hz, Table 2) due to the fact that it is farther from the quinoline region.

The above interaction models allowed us to establish that, in the two complexes, the enantiodiscrimination must be mainly determined by the different relative positions of the methyl group of **3** and of the methyl group of the 1-(1-naphthyl)ethyl moiety of **1**: in the **1**/(*S*)-**3** pair these are *transoid*, in the **1**/(*R*)-**3** one they are *cisoid* and, hence, generate a steric repulsive interaction (Fig. 7).

Even though the interactions involved both in the stabilization of the diastereoisomeric adducts and in their enantiodifferentiation are very weak (see association constants values), the starting conformation of the carbamate quinine determines a highly anisotropic pocket, included between the quinoline and carbamate functions, which is responsible for the chemical shift differentiation.

The NOE effects detected in the **2**/(*S*)-**3** mixture are as follows: dipolar interactions between the dinitrophenyl protons of **3** and the $H_3$ and $H_4$ quinoline protons of **2** (Fig. 8a) and between the carbamate NH and CH protons of **2** and the NH proton of (*S*)-**3** (Fig. 8b). Perturbation of the proton $H_8$ of **2** enhances the resonance $H_o$, $H_p$ and NH of (*S*)-**3** (Fig. 8c), but the effect on the proton $H_o$ is strongly prevailing.

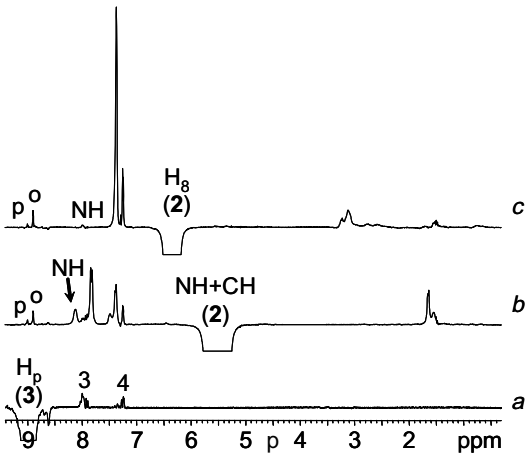


**Figure 8.** $^1H\{^1H\}$-NOE difference spectra (300 MHz, $CDCl_3$, 25 °C) of equimolar mixture (*S*)-**3**/**2** (120 mM) corresponding to the saturation of $H_p$ (a) proton of (*S*)-**3** and of NH + CH (b) and $H_8$ (c) protons of **2**.

Therefore, we can conclude that (*S*)-**3** is included between the quinoline and naphthalene rings, but being closer to the first with respect to the latter. The change of its orientation with respect to the previous cases is simply the consequence of the different stereochemistries of **2** with respect to **1**. In fact (*S*)-**3** keeps the same kind of relative orientation with respect to the carbamate function of **2**, having the 3,5-dinitrophenyl moiety parallel to the naphthalene ring and its NH proton directed towards the hydrogen bond acceptor sites of the carbamate moiety, that is, the oxygen and the carbonyl (Fig. 9).

Therefore, the groups bound to the stereogenic centre of (*S*)-**3** must be external to the region included between the two aromatic rings of the chiral auxiliary.

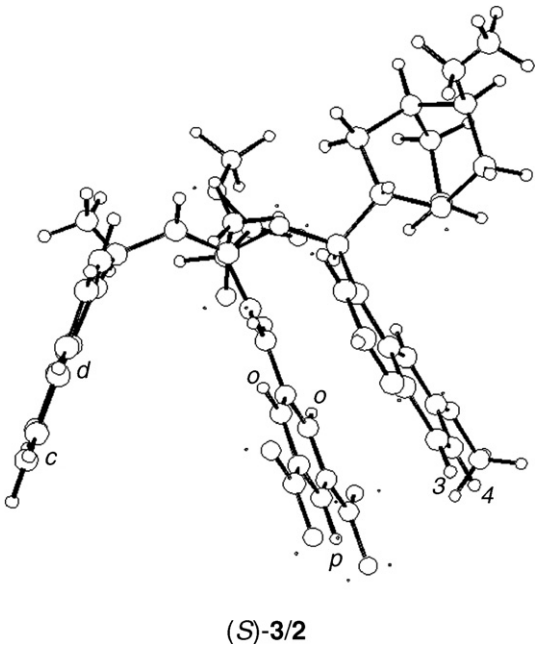


**Figure 9.** Graphical representation of the diastereoisomeric complex (*S*)-**3**/**2**.

Analogous NOEs are detected in the other mixture **2**/(*R*)-**3** suggesting a relative stereochemical arrangement similar to that found for **2**/(*S*)-**3**.

The two complexes, having very similar association constants, are also slightly differentiated in the NMR spectra probably due to the fact that the groups bound to the stereogenic centres of (*S*)- and (*R*)-**3** are endowed with a more pronounced conformational freedom, in addition to the fact that these groups do not feel significant anisotropic effects produced by aromatic rings.

Stochastic dynamic simulations of the enantioselective complex between the *anti*-**1** and the enantiomers of *N*-(3,5-dinitrobenzoyl) alanine methyl ester were carried out, starting from the *anti*-**1** NMR determined conformation, after a minimization, whereas an extensive conformational search followed by a minimization was carried out on the *N*-(3,5-dinitrobenzoyl)alanine methyl ester.

For all the simulations, chloroform was set as the solvent to allow the comparison with the NMR data. During the annealing simulation, 1000 structures were sampled over time along the trajectory. In accordance with the NMR results, both complexes showed the 3,5-dinitrophenyl ring of the alanine derivative enantiomers included in the pocket formed by the quinuclidine and the naphthyl moieties of **1** (Figs. 10 and 11).

In order to inspect the possibility of π–π stacking interactions, the center-to-ring center distances between two dummy atoms (aromatic ring centroids) of the

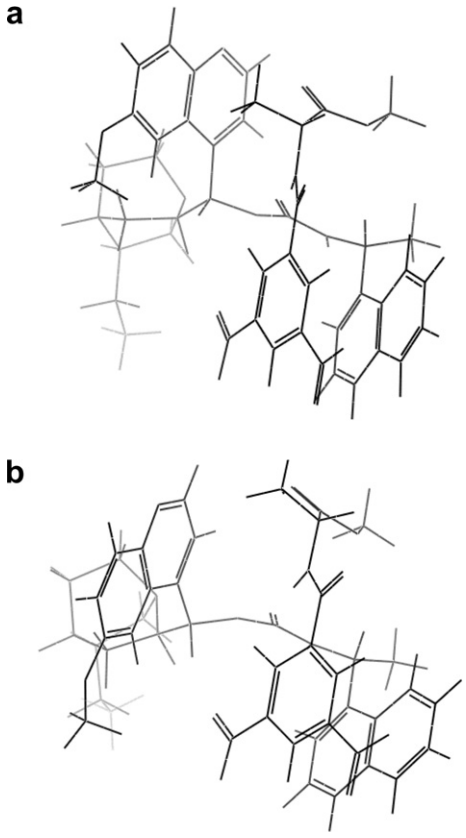


**Figure 10.** Representation of **1**/(*S*)-**3** complex with the highest energy (a) and with the lowest energy (b) content from the annealing.

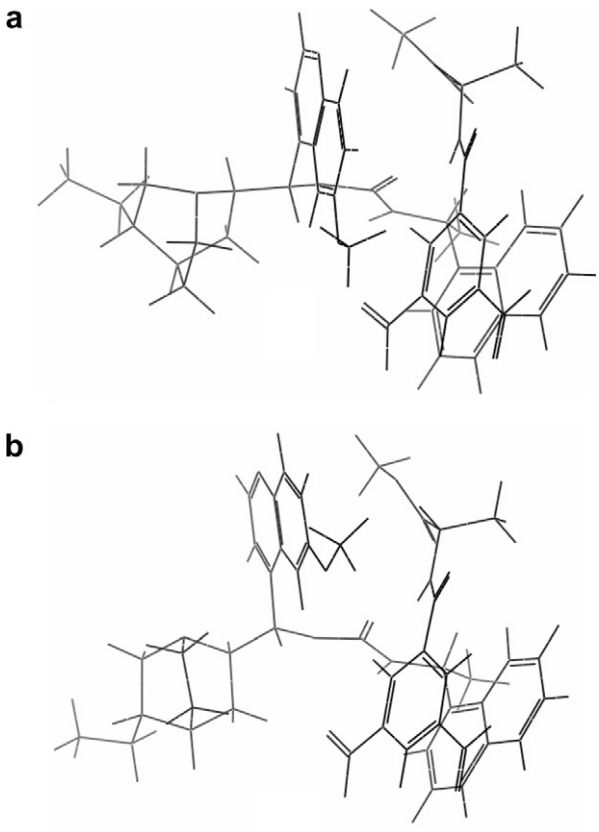


**Figure 11.** Representation of **1**/(*R*)-**3** complex with the highest energy (a) and with the lowest energy (b) content from the annealing.

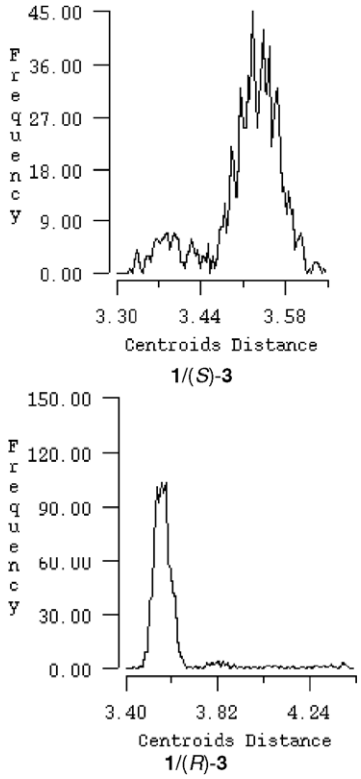


**Figure 12.** Distributions of intermolecular distances between dummy atoms placed at ring centroids of *N*-(3,5-dinitrobenzoyl)alanine methyl ester enantiomers and 9-*O*-[(*S*)-1-(1-naphthyl)ethylcarbamate]dihydroquinine, encountered during the simulation time period in chloroform.

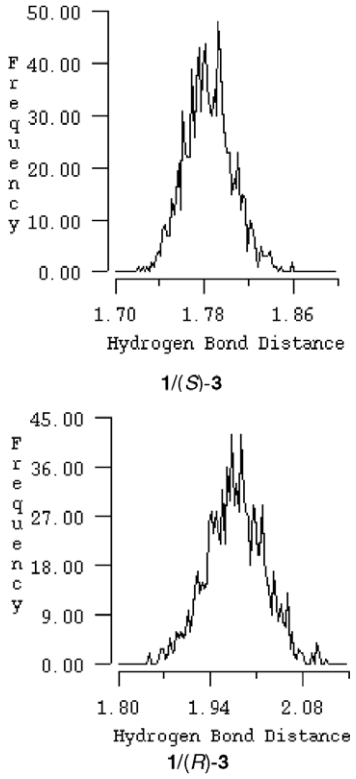


**Figure 13.** Distributions of H-bond distances between the NH proton of *N*-(3,5-dinitrobenzoyl)alanine methyl ester enantiomers and the oxygen of the carbonyl function of the carbamate of 9-*O*-[(*S*)-1-(1-naphthyl)ethylcarbamate]dihydroquinine, encountered during the simulation time period in chloroform.

3,5-dinitrophenyl ring of (*S*)-**3**/(*R*)-**3** and the naphthyl moiety of **1**, respectively, were monitored and plotted (Fig. 12). In both cases, it is evident that the two adducts are stabilized by a parallel-displaced π–π interaction.[8] Moreover it is clear from the intermolecular distances distribution plots (Fig. 13) between the NH group of *N*-(3,5-dinitrobenzoyl)alanine methyl ester and the oxygen of the dihydroquinine carbamate moiety, that an additional stabilizing interaction takes place between the NH group of the *N*-(3,5-dinitrobenzoyl)alanine methyl ester enantiomers and the carbonyl oxygen of *anti*-**1**.

A potential energy difference of about 16 kJ/mol was found (Fig. 14) between the examined complexes, showing that complex **1**/(*R*)-**3** should be the most stable one. The discrepancy between this result and the calculated NMR association constants according to which the strongest complex is **1**/(*S*)-**3**, could be due to the solvent explicit effect in NMR experiments. MacroModel treats the solvent as a fully equilibrated analytical continuum starting near the van der Waals surface of the solute (GB/SA model). On the contrary, $CDCl_3$ molecules could interact with the complexes in the NMR measurements thus influencing the measured association constants. Of course the values of the energies obtained from force field calculations might reflect the fact that the parameters used in the MD simulations are insufficient for accurate calculation of the complexation energies.

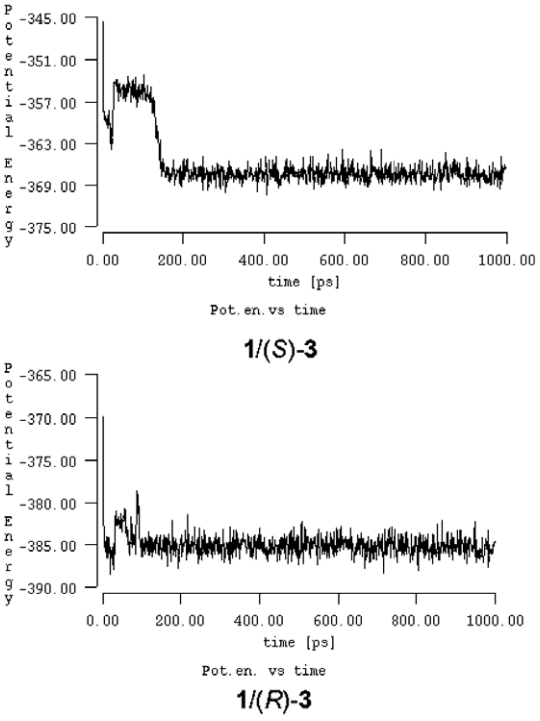


**Figure 14.** Trajectories of the potential energies for the complexes over the 1 ns simulation time period in chloroform.

## 3. Conclusions

A few years ago,[2a] we studied the ability of quinine C9 carbamates to differentiate enantiomeric substrates endowed with two hydrogen-bond donor groups and to address towards different interaction pathways exploiting both the potentialities of its carbamate function and the base properties of quinuclidine nitrogen. In this case, the multireceptorial character of quinine and quinine derivatives was highlighted.

Here, we complete the picture of the enantiodiscriminating potentialities of C9 carbamates of dihydroquinines in two respects, in particular, the molecular basis of the enhanced enantiodiscriminating efficiency of C9 derivatives containing the (*S*)-1-(1-naphthyl)ethyl carbamate group and looking for the origin of enantiodiscrimination when the chiral analyte, *N*-(3,5-dinitrobenzoyl)alanine methyl ester has only one hydrogen-bond donor group, the amide function.

In this last case, the stabilization of the diastereoisomeric adducts completely rely on the carbamate function, which guarantees attractive interactions involving its π-donor naphthalene ring and the π-acidic aromatic moiety of the 3,5-dinitrophenyl groups of the two enantiomers, assisted by the attractive hydrogen bond interactions between the amidic and estereal moieties of the amino acid derivative and the carbamate function of the chiral selector. The quinuclidine nitrogen is not involved at all and, consequently, the chiral auxiliary retains both in the two diastereoisomeric adducts in its *closed* conformation.

The orientation of the enantiomeric pairs inside the diastereoisomeric complexes is controlled by the carbamate naphthyl group of **1** and **2**: enantiomeric substrates always dispose their π-acidic ring parallel to the naphthalene ring and the amidic function bound to it is directed towards the carbamate polar groups. In this way, when the naphthalene and quinoline rings have *anti* arrangements, as in **1**, the groups bound to the stereogenic centre of the amino acid are constrained in proximity both of the C9 stereogenic centre of the chiral auxiliary and of its quinoline ring and enhanced differential anisotropic effects of methyl groups are produced, which are the basis of their high NMR enantiodiscrimination.[2d] When the carbamate stereogenic centre has an (*R*)-absolute configuration, as in **2**, *syn*-naphthalene and quinoline rings are determined while the methyl groups bound to the stereogenic centre of the enantiomeric mixture are far away from the C9 and quinoline moieties, resulting in a lower enantiodiscrimination.

From the MD (molecular dynamics) of **1**/(*S*)-**3** complex we observed the same features as from the NMR studies: the π–π interaction between the 3,5-dinitrophenyl moiety of (*S*)-**3** and the naphthalene of the dihydroquinine carbamate function, the H-bond between the NH proton of (*S*)-**3** and the oxygen of the carbonyl function of the carbamate. The same applies to the complex **1**/(*R*)-**3**. Overall, the complexes found by molecular dynamics resemble quite well those determined by NMR. We believe that the rigidity of the quinine system was crucial in such an agreement being obtained. Systems that are more flexible have greater sensitivity to accurate force field parameters and conformational search protocols employed.

Gathering together the present NMR results with our previous researches[2a] on the same matter with the support of computational studies leads to the root of the enantiodiscrimination mechanism by quinine and dihydroquinine C9 carbamates, allowing to attain a comprehensive rationalization of chiral discrimination phenomena. The described study gives some insight into the various energetic contributions to the total binding free energy. The whole complexation is given by a global sum of very weak contributions except for the hydrogen bond stabilizations. In fact, this related class of interactions represents the most important and most conserved energy contribution between host and guest. Stacking and other charge transfer interactions are smaller and provide various stabilizations. However, the sum of these interactions results in an energy gain, which may affect the enantioselective discrimination. Thus integrating standard experimental protocols by computational methods[9–11] for screening chiral auxiliaries enantioselective potential constitutes a very attractive approach.

## 4. Experimental

### 4.1. General methods

NMR measurements were performed on a spectrometer operating at 300 MHz for $^1$H and the temperature was controlled to ±0.1 °C. All the $^1$H NMR chemical shifts are referenced to TMS as external standard. The 2D NMR spectra were obtained by using standard sequences. The double-quantum-filtered (DQF) COSY experiments were recorded with the minimum spectral width required; 512 increments of 8 scans and 2K data points were acquired. The relaxation delay was 5 s. The data were zero-filled to 2K × 1K and a Gaussian function was applied for processing in both dimensions. The NOESY (Nuclear Overhauser and Exchange SpectroscopY) spectra were recorded in the phase-sensitive mode, by employing a mixing time of 0.6 s. The spectral width used was the minimum required in both dimensions. The pulse delay was maintained at 8 s; 512 hypercomplex increments of 8 scans and 2K data points each were collected. The data matrix was zero-filled to 2K × 1K and a Gaussian function was applied for processing in both dimensions. The $^1$H{$^1$H}-NOE experiments were performed in the difference mode. The decoupler power used was the minimum required to saturate the spin of interest. A waiting time of 10 s was used to allow the system to reach the equilibrium. Each NOE experiment was repeated at least four times.

In the association constant determinations, the non-linear fitting of chemical shifts data on the basis of Eq. 1, which correlates chemical shifts to the initial concentrations, was performed by using KaleidaGraph 3.09.

$$C_0 = \frac{(\delta_{obs} - \delta_F)(\delta_B - \delta_F)}{K(\delta_B - \delta_{obs})^2} \quad (1)$$

Eq. 1 is obtained by combining Eq. 2 of the observed chemical shift ($\delta_{obs}$) in fast exchanging conditions to the expression of the association constant $K$ (Eq. 3),

$$\delta_{obs} = \delta_F X_F + \delta_B X_B \quad (2)$$

where $\delta_F$ and $\delta_B$ are the chemical shifts of the free and bound species, and $X_F$ and $X_B$ are their molar fractions.

$$K = \frac{X_B}{C_0(1 - X_B)} \quad (3)$$

The stoichiometries were determined[6] by analyzing solutions prepared by mixing different volumes of stock solutions of each component having the same molar concentration $M$ to obtain a prefixed volume $V$ directly in the NMR tube.

The stereochemical representations were obtained with PCModel 6.0 program (MMx force field).

### 4.2. Computational methods

All the modelling studies were carried out on a SGI-OCTANE operating under IRIX 6.5.+ using the softwares MacroModel (version 9.1)[11] as implemented in the version 7.5 of the MAESTRO[11] suite and FLO+ (Version April03).[10] Two different NMR determined starting conformations ((*S*)-**3**/(*R*)-**3**) were used for the AMBER* conformational searches in chloroform as the solvent (normal cutoff, 1000 iterations, 1000 maximum number of steps) with the PRCG algorithm, until a gradient of 0.001 kJ/Å mol was reached. Least squares superposition of all the non-hydrogen atoms was used to eliminate duplicate conformations. All AMBER* force field equations are identical to those of authentic AMBER from Kollman. The MacroModel default for hydrogen bonding uses the Kollman's 6,12-Lennard Jones treatment and an improved peptide backbone parameter set.[12] An energy window of 20 kJ/mol above the global minimum was set for saving conformations. Starting conformations were first minimised using the MacroModel minimization routine with the same parameters.

Systems were prepared manually and saved as .pdb files by placing the lowest energy conformer of the chiral substrate near the carbamate quinine **1** in a position similar to that observed in the NMR spectra, by the software FLO+ (Version April03).[10]

The .pdb files were read by MacroModel (version 9.1)[11] and minimized using the above parameters, except for the convergence threshold, for which the default value was left (0.05 kJ $Å^{-1}$). Full molecular dynamics (MD) with simulated annealing was then performed for each complex, using the stochastic dynamics method to simulate the random collisions with solvent as well as solvent friction forces.[13] The SHAKE[14] protocol was activated using a time step of 1 fs. A cooling protocol from 298 to 10 K was applied (10 ps equilibrium run at 298 K, 100 ps simulation coupled to a thermal bath of 150 K for data collection). The system was finally cooled to 10 K for 1000 ps. Conformations from each MD annealing trajectory (1000 structures) were sampled. The distance between the NH proton of the chiral substrate and the oxygen of the quinine carbamate moiety was monitored during the simulation and plotted by the MacroModel Plot Tool (version 9.1).[11]

### 4.3. Materials

9-*O*-[(*S*)- and (*R*)-1-(1-naphthyl)ethylcarbamate]dihydroquinine were prepared according to Ref. 2b.

**4.3.1. 9-*O*-[(*S*)-1-(1-Naphthyl)ethylcarbamate]dihydroquinine 1.** $^1$H NMR (300 MHz, $CDCl_3$, 25 °C, 120 mM) of *anti*-**1**: $\delta$ 8.72 ($H_2$, d, $J = 3.6$ Hz), 8.08 ($H_g$, d, $J = 7.0$ Hz), 7.99 ($H_3$, d, $J = 9.3$ Hz), 7.78 ($H_c$, d, $J = 7.4$ Hz), 7.50 ($H_f$, br dd), 7.49 ($H_5$, br d), 7.47 ($H_a$, br d), 7.45 ($H_d$, d, $J = 7.0$ Hz), 7.41 ($H_b$, br dd), 7.35 ($H_1$, d, $J = 3.6$ Hz), 7.34 ($H_4$, br dd), 7.33 ($H_e$, br dd), 6.49 ($H_8$, d, $J = 7.0$ Hz), 5.59 (CH, dq, $J = 7.7$ Hz, $J = 7.0$ Hz), 5.16 (NH, d, $J = 7.7$ Hz), 3.93 (OMe, s), 3.25 ($H_9$, m), 3.06 ($H_{15}$, m), 2.95 ($H_{19}$, m), 2.57 ($H_{14}$, m), 2.56 ($H_{16}$, m), 2.31 ($H_{18}$, m), 1.71 ($H_{10}$, m), 1.70 ($H_{12}$, m), 1.57 (Me, d, $J = 6.5$ Hz), 1.48 ($H_{11}$, m), 1.38 ($H_{17}$, m), 1.36 ($H_{13}$, m), 1.29 ($CH_2CH_3$, m), 0.78 ($CH_2CH_3$, t, $J = 7.0$ Hz). $[\alpha]_D^{25} = -6.8$ ($c$ 1, $CHCl_3$).

$^1$H NMR (300 MHz, $CDCl_3$, 25 °C, 120 mM) of *syn*-**1**: $\delta$ 8.16 ($H_2$), 8.01 ($H_g$), 6.39 ($H_8$), 6.00 ($H_1$), 5.55 (CH), 5.16 (NH), 3.84 (OMe), 2.96 ($H_9$).

**4.3.2. 9-*O*-[(*R*)-1-(1-Naphthyl)ethylcarbamate]dihydroquinine 2.** $^1$H NMR (300 MHz, $CDCl_3$, 25 °C, 120 mM) of *anti*-**2**: $\delta$ 8.63 ($H_2$, d, $J = 4.5$ Hz), 7.97 ($H_3$, d, $J = 9.3$ Hz), 7.81 ($H_g$, d, $J = 7.8$ Hz), 7.80 ($H_c$, d, $J = 9.0$ Hz), 7.73 ($H_d$, d, $J = 7.7$ Hz), 7.41 ($H_b$, br dd), 7.39 ($H_5$, d, $J = 2.8$ Hz), 7.37 ($H_a$, br d), 7.33 ($H_e$, br dd), 7.31 ($H_4$, dd, $J = 9.3$ Hz, $J = 2.8$ Hz), 7.27 ($H_f$, br dd), 7.24 ($H_1$, d, $J = 4.5$ Hz), 6.44 ($H_8$, d, $J = 7.0$ Hz), 5.55 (CH, dq, $J = 7.7$ Hz, $J = 6.5$ Hz), 5.16 (NH, d, $J = 7.7$ Hz), 3.74 (OMe, s), 3.25 ($H_9$, m), 3.07 ($H_{15}$, m), 3.00 ($H_{19}$, m), 2.60 ($H_{16}$, m), 2.30 ($H_{18}$, m), 1.75 ($H_{12}$, m), 1.71 ($H_{10}$, m), 1.66 ($H_{14}$, m), 1.64 (Me, d, $J = 6.5$ Hz), 1.53 ($H_{11}$, m), 1.42 ($H_{13}$, m), 1.38 ($H_{17}$, m), 1.29 ($CH_2CH_3$, m), 0.81 ($CH_2CH_3$, t, $J = 7.0$ Hz). $[\alpha]_D^{25} = +16.05$ ($c$ 1, $CHCl_3$).

$^1$H NMR (300 MHz, $CDCl_3$, 25 °C, 120 mM) of *syn*-**2**: $\delta$ 8.71 ($H_2$), 8.08 ($H_g$), 7.97 ($H_3$), 6.25 ($H_8$), 5.62 (CH), 5.16 (NH), 3.88 (OMe), 2.75 ($H_9$, $H_{15}$, $H_{19}$), 2.30 ($H_{16}$), 1.98 ($H_{18}$), 1.49 (Me), 0.67 ($CH_2CH_3$).

## Acknowledgments

The work was supported by MIUR (Project 'High performance separation systems based on chemo- and stereoselective molecular recognition' grant 2005037725 and FIRB Project RBPR05NWWC) and ICCOM-CNR. The Schrodinger, Inc. support service[11b] and Dr. Joseph M. Hayes (Structural Biology and Chemistry Group, Institute of Organic and Pharmaceutical Chemistry, The National Hellenic Research Foundation, Athens,

Greece) are gratefully acknowledged for the helpful discussion and suggestions provided on the centroid distance calculation.

## References


1. (a) Maier, N. M.; Lindner, W. Methods and Priciples in Medicinal Chemistry. In *Chirality in Drug Research*; Francotte, E., Lindner, W., Eds.; WILEY-WCH, 2006; Vol. 33, Chapter 7 (b) Lammerhofer, M.; Franco, P.; Lindner, W. *J. Sep. Sci.* **2006**, *29*, 1486–1496.
2. (a) Uccello-Barretta, G.; Balzano, F.; Quintavalli, C.; Salvadori, P. *J. Org. Chem.* **2000**, *65*, 3596–3602; (b) Uccello-Barretta, G.; Bardoni, S.; Balzano, F.; Salvadori, P. *Tetrahedron: Asymmetry* **2001**, *12*, 2019–2023, In Figure 1 an interchange between the structures of **1e** and **1f** was made; (c) Uccello-Barretta, G.; Mirabella, F.; Balzano, F.; Salvadori, P. *Tetrahedron: Asymmetry* **2003**, *14*, 1511–1516; (d) Uccello-Barretta, G.; Balzano, F.; Salvadori, P. *Chirality* **2005**, *17*, S243–S248.
3. Uccello-Barretta, G.; Di Bari, L.; Salvadori, P. *Magn. Reson. Chem.* **1992**, *30*, 1054–1063.
4. Smith, B. D.; Goodenough-Lashua, D. M.; DeeAnne, M.; D'Souza, C. J. E.; Carlisle, J. E.; Norton, K. J.; Schmidt, L. M.; Tung, J. C. *Tetrahedron Lett.* **2004**, *45*, 2747–2749.
5. (a) Karplus, M. *J. Chem. Phys.* **1959**, *30*, 11–15; (b) Karplus, M. *J. Am. Chem. Soc.* **1963**, *85*, 2870–2871; (c) Govil, G.; Hosur, R. V. In *Conformation of Biological Molecules: Results from NMR*. In *NMR: Basic Principles and Progress*; Springer, 1982; Vol. 20.
6. (a) Job, P. *Ann. Chem.* **1928**, *9*, 113–134; (b) Homer, J.; Perry, M. *J. Chem. Soc., Faraday Trans. 1* **1986**, *82*, 533–543.
7. Fielding, L. *Tetrahedron* **2000**, *56*, 6151–6170.
8. (a) McGaughey, G. B.; Gagnè, M.; Rappe, A. K. *J. Biol. Chem.* **1998**, *273*, 15458–15463; (b) Chelli, R.; Gervasio, F. L.; Procacci, P.; Schettino, V. *J. Am. Chem. Soc.* **2002**, *124*, 6133–6143.
9. Ragusa, A.; Hayes, J. M.; Light, M. E.; Kilburn, J. D. *Eur. J. Org. Chem.* **2006**, *16*, 3545–3549.
10. (a) McMartin, C.; Bohacek, R. S. *J. Comput-Aided Mol. Des.* **1997**, *11*, 333–344; (b) QXP is the molecular mechanics module in FLO+ (version April03), a molecular design program commercially available from: Colin McMartin, Thistlesoft, PO Box 227, Colebrook, CT 06021, USA.
11. (a) Mohamadi, F.; Richards, N. G. J.; Guida, W. C.; Liskamp, R.; Lipton, M.; Caufield, C.; Chang, G.; Hendrickson, T.; Still, W. C. *J. Comput. Chem.* **1990**, *11*, 440–467; (b) Schrodinger, L. L. C. New York, NY, 2005.
12. (a) Ferguson, D. M.; Kollman, P. A. *J. Comput. Chem.* **1991**, *12*, 620–626; (b) McDonald, D. Q.; Still, W. C. *Tetrahedron Lett.* **1992**, *33*, 7743–7746.
13. (a) Maier, N. M.; Schefzick, S.; Lombardo, G. M.; Feliz, M.; Rissanen, K.; Lindner, W.; Lipkowitz, K. B. *J. Am. Chem. Soc.* **2002**, *124*, 8611–8629; (b) Hellriegel, C.; Skogsberg, U.; Albert, K.; Läemmerhofer, M.; Maier, N. M.; Lindner, W. *J. Am. Chem. Soc.* **2004**, *126*, 3809–3816.
14. Ryckaert, J. P.; Ciccotti, G.; Berendsen, H. J. C. *J. Comput. Phys* **1977**, *23*, 327–341.